organic compounds

Ring conformations and inter-molecular interactions in two fused dibenzoazocines

Andrés F. Yepes,[a] Ederson Jaimes,[a] Ali Bahsas,[b] Alirio Palma,[a] Michael B. Hursthouse,[c] Justo Cobo[d] and Christopher Glidewell[e]*

[a]Laboratorio de Síntesis Orgánica, Escuela de Química, Universidad Industrial de Santander, AA 678 Bucaramanga, Colombia, [b]Laboratorio de RMN, Grupo de Productos Naturales, Departamento de Química, Universidad de los Andes, Mérida 5101, Venezuela, [c]School of Chemistry, University of Southampton, Highfield, Southampton SO17 1BJ, England, [d]Departamento de Química Inorgánica y Orgánica, Universidad de Jaén, 23071 Jaén, Spain, and [e]School of Chemistry, University of St Andrews, Fife KY16 9ST, Scotland

Correspondence e-mail: cg@st-andrews.ac.uk

5-Acetyl-2-chloro-8,11-dimethyl-5,6,11,12-tetrahydrodi-benzo[b,f]azocine, $C_{19}H_{20}ClNO$, (I), crystallizes as a single fully ordered isomer, but 14-acetyl-8,11-dimethyl-7,8,13,14-tetrahydrobenzo[f]naphtho[1,2-b]azocine–14-acetyl-8,9-di-methyl-7,8,13,14-tetrahydrobenzo[f]naphtho[1,2-b]azocine (74/26), $C_{23}H_{23}NO$, (II), exhibits threefold whole-molecule disorder involving both configurational and structural isomers. In (I) and in the predominant form of (II), the azocine rings adopt very similar conformations, forming boat-shaped rings having approximate twofold rotational symmetry. There are no direction-specific intermolecular interactions in the crystal structure of (I), but the molecules of (II) are weakly linked into chains by an aromatic π–π stacking interaction. The compounds were made under green conditions using an acid-catalysed cyclization process having very high atom utilization.

Comment

We are interested in developing the intramolecular Friedel–Crafts reaction as a versatile route to the construction of nitrogen-containing heterocycles, and thus in the application of this methodology to the synthesis of both tetrahydro-dibenzo[b,f]azocines and tetrahydrobenzo[f]naphtho[1,2-b]-azocines. We describe here the preparation of 5-acetyl-2-chloro-8,11-dimethyl-5,6,11,12-tetrahydrodibenzo[b,f]azocine, (I) (Fig. 1), and 14-acetyl-8,11(8,9)-dimethyl-7,8,13,14-tetra-hydrobenzo[f]naphtho[1,2-b]azocine, (II) (Fig. 2), by treat-ment of the corresponding N-acetyl-2-allyl-N-benzyl-4-chloroaniline and N-acetyl-2-allyl-N-benzyl-1-naphthylamine, respectively, with polyphosphoric acid (PPA) (see scheme). We report the structures of (I) and (II) and compare the

conformations of these compounds with that of the related azocine derivative 5-acetyl-10b,11,12,13,14,14a-hexahydro-11,14-methanotribenzo[b,d,f]azocin-6-one, (III) [Cambridge Struc-tural Database (Allen, 2002) refcode OMAZOR; Bocelli et al., 2002], the structure of which (see scheme) was reported on a proof-of-constitution basis. The syntheses of (I) and (II) proceed with high atom utilization (see scheme), whereas the synthesis reported for (III) requires both a palladium-based reagent and an iodinated aryl precursor, such that both of the expensive constituents, viz. Pd and I, are discarded during the synthesis. In addition to the general advantages of the present synthetic approach in terms of both cost and atom efficiency, the rigorous purification necessary for synthetic products aimed at possible pharmaceutical applications should be much more straightforward in the absence of toxic heavy metals.
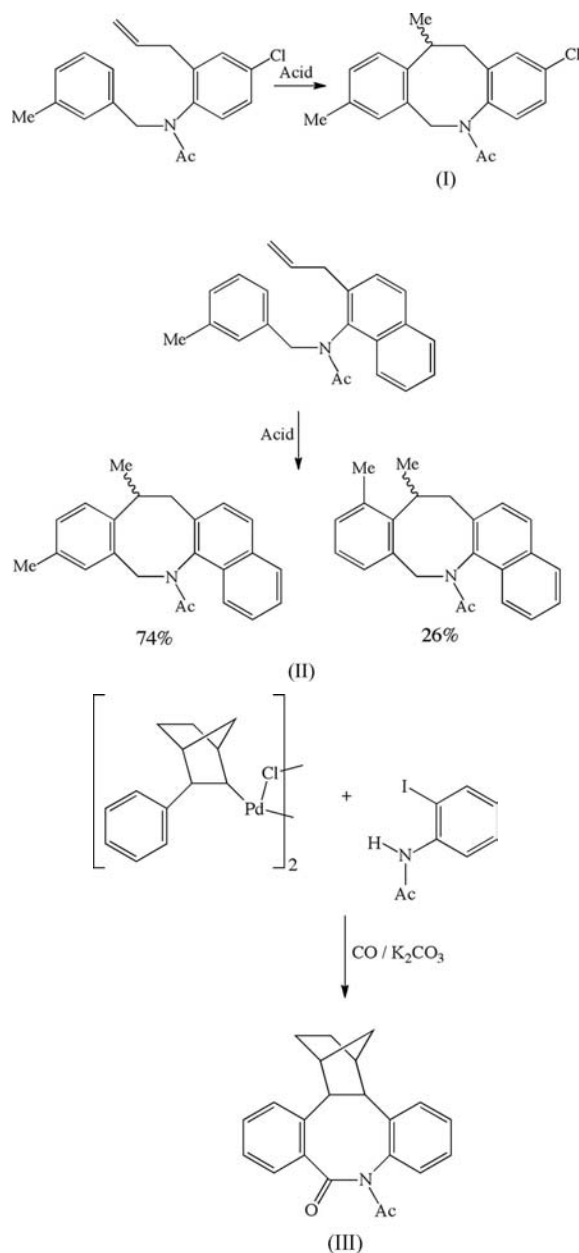
When the precursor benzylamine carries a substituent in the 3-position of the benzyl ring, the intramolecular Friedel–
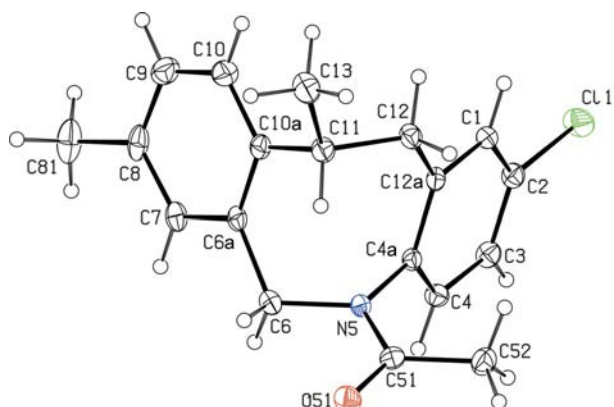
doi:10.1107/S0108270110014708

Figure 1
The molecular structure of (I), showing the atom-labelling scheme. Displacement ellipsoids are drawn at the 30% probability level and H atoms are shown as small spheres of arbitrary radii.

Crafts reaction can, in principle, occur at a choice of sites, leading to two possible locations for that substituent in the final azocine product. It was evident form the ^{1}H and ^{13}C

NMR spectra, measured in chloroform solution, that compound (I) had been formed as a single regioisomer (cf. Fig. 1), but that compound (II) has been formed as a mixture of two regioisomers, with 14-acetyl-8,11-dimethyl-7,8,13,14-tetrahydrobenzo[f]naphtho[1,2-b]azocine as the major product and 14-acetyl-8,9-dimethyl-7,8,13,14-tetrahydrobenzo[f]-naphtho[1,2-b]azocine as the minor product, with a product ratio of approximately 2.8:1. All attempts to separate these isomeric products, either by chromatography or by fractional crystallization, proved unsuccessful. There are three distinct isomeric forms in the disorder model and these are conveniently denoted forms A–C. In form A, containing atom O141 (Fig. 2a), there is a methyl substituent at position C11 of the fused benzene ring and, in the selected asymmetric unit, the reference molecule has an R configuration at the stereogenic atom C8. Form B, containing atom O441 (Fig. 2b) is the S enantiomer of form A, and form C, containing atom O641 (Fig. 2c), is a structural isomer of form A, with the methyl substituent at atom C59 rather than C61, but again with an R configuration at atom C58. These three disorder components
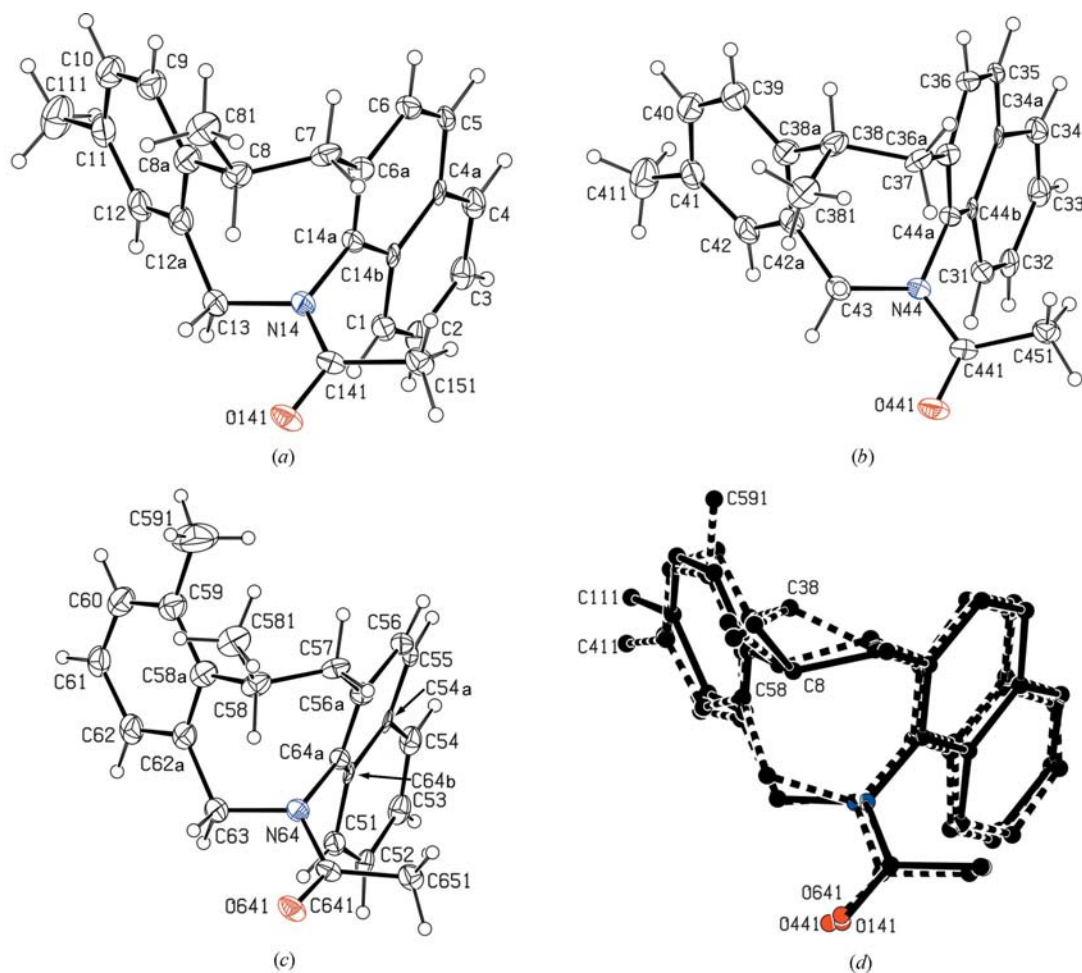

Figure 2
The molecular components of (II), showing the atom-labelling scheme for (a) isomer A, (b) isomer B, (c) isomer C and (d) an overlay of all three disorder components. In parts (a)–(c), displacement ellipsoids are drawn at the 30% probability level and H atoms are shown as small spheres of arbitrary radii. In part (d), atoms are drawn as spheres of arbitrary radii and the H atoms have all been omitted. This part is oriented to show the S configuration at atom C38, as opposed to the R configuration at atoms C8 and C58, and the locations of the methyl C atoms C111, C411 and C591.
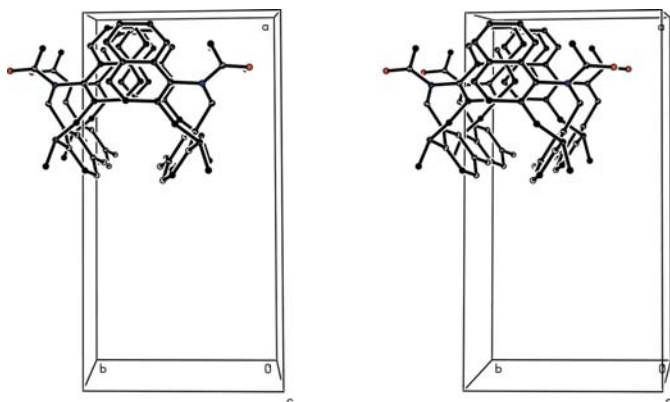
organic compounds

Figure 3
A stereoview of part of the crystal structure of (II), showing the formation of a chain of π-stacked molecules running parallel to the [001] direction. For the sake of clarity, only the major disorder component is shown and H atoms have all been omitted.

occupy similar sets of atomic sites (Fig. 2d) and the refined site occupancies for forms *A–C* are 0.634 (6), 0.107 (3) and 0.260 (5), respectively. Hence, averaged over the entirety of the crystal selected for data collection, some 89.4% of the reference molecules have an *R* configuration and 10.7% have an *S* configuration. Similarly, in some 74.1% of the molecules, the methyl location corresponds to that observed in (I). No evidence was found for any significant population of the reference site by the *S* enantiomer of form C. The centrosymmetric space group accommodates equal numbers of the two enantiomeric forms of each of the structural isomers identified here, so that, overall, (II) crystallizes as a mixture of two structural isomers, each of which is racemic. This inherent ambiguity in the final location of a 3-substituent in this ring of the precursor molecule necessarily introduces a modest limitation to the general utility of this synthetic approach.

The eight-membered rings in (I) and (II) have very similar conformations, readily illustrated by a comparison of the corresponding torsion angles around the rings (Table 2), noting that the chemical numbering schemes used for (I) and (II) mean that corresponding atoms in the two compounds often carry different labels (Figs. 1 and 2). These torsion angles demonstrate an approximate local twofold rotation symmetry for the topology of the eight-membered rings, the overall shape of which in each compound is reminiscent of the D_{2d} ($\overline{4}2m$) boat configuration found in cyclooctatetraene, C_8H_8, both in the gas phase (Traetteberg, 1966) and in the crystalline state (Claus & Krüger, 1988).

Compound (III) (Bocelli *et al.*, 2002) exhibits a somewhat different conformation in its eight-membered ring, as indicated by the corresponding torsion angles (Table 3), listed in the same order as those for (I) and (II) (Table 2), but noting here that the atom-numbering scheme employed for (III) by the original authors was an arbitrary one. The difference between (III) on the one hand and (I) and (II) on the other is possibly a consequence of the additional ring fusion present in (III). Nonetheless, the general pattern of the signs of the torsion angles in (III) corresponds with those in (I) and (II), with again an approximate local twofold rotational symmetry,
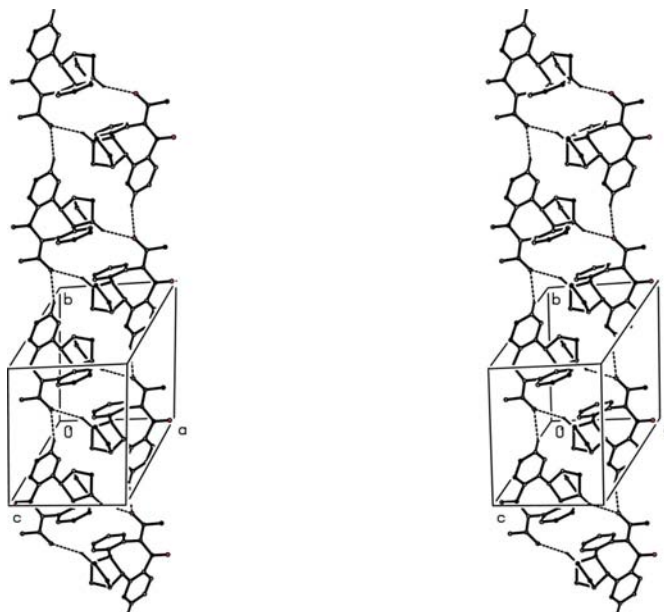

Figure 4
A stereoview of part of the crystal structure of (III) (CSD refcode OMAZOR; Bocelli *et al.*, 2002), showing the formation of a chain of centrosymmetric $R_2^2(16)$ and $R_4^2(18)$ rings along [010]. For the sake of clarity, H atoms not involved in the motifs shown have been omitted.

although the magnitudes of several of the pairs are very different in (III). In particular for (III), the pair of torsion angles C20—C25—C1—C16 and C8—C13—C14—N1, and the pair C25—C1—C6—C8 and C13—C14—N16—C20, have values markedly different from the corresponding torsion angles in (I) and (II).

The bond distances in (I) exhibit no unusual values, but in (II) the distances within the naphthalene system clearly show evidence of the type of bond fixation found in naphthalene itself (Capelli *et al.*, 2006; Fabbiani *et al.*, 2006), with the bonds C1—C2, C3—C4, C5—C6 and C6a—C14a in the major form *A* lying in the range 1.364 (4)–1.377 (3) Å, all significantly shorter than the rest of the peripheral C—C distances in this unit, which range from 1.409 (3) to 1.424 (5) Å (Table 1).

The crystal structures of (I) and (II) contain neither C—H···*X* (*X* = N or O) nor C—H···π(arene) hydrogen bonds. While aromatic π–π stacking interactions are absent from the structure of (I), there is a weak interaction of this type in (II), where we consider only the major form *A*. The ring C1–C4/C4a/C14b in the form *A* molecule at (*x, y, z*) makes a dihedral angle of 14.7 (2)° with the ring C4a/C5/C6/C6a/C14a/C14b in the corresponding molecule at (*x*, $\frac{3}{2}$ − *y*, $-\frac{1}{2}$ + *z*). The ring-centroid separation is 3.747 (10) Å, with a perpendicular distance of one ring centroid from the opposing plane of *ca* 3.35 Å, corresponding to a ring-centroid offset of *ca* 1.68 Å. By this means, molecules related by the *c*-glide plane at *y* = $\frac{3}{4}$ are weakly linked into a π-stacked chain running parallel to the [001] direction (Fig. 3). Two chains of this type, related to one another by inversion, pass through each unit cell, but there are no direction-specific interactions between adjacent chains.

By contrast, the crystal structure of (III) contains two C—H···O hydrogen bonds, one of them rather long, but neither the structural effect of these nor even their occurrence was mentioned in the original report (Bocelli *et al.*, 2002). The co-operative action of these two hydrogen bonds generates a chain of fused centrosymmetric rings running parallel to the [010] direction, in which $R_2^2(16)$ rings (Bernstein *et al.*, 1995) centred at $(\frac{1}{2}, n + \frac{1}{2}, \frac{1}{2})$, where *n* represents an integer, alternate with $R_4^2(18)$ rings centred at $(\frac{1}{2}, n, \frac{1}{2})$, where *n* again represents an integer (Fig. 4). It is of interest to note that both hydrogen bonds in (III) involve the acetyl O atom as the acceptor, so accounting for the $R_4^2(18)$ motif of one of the rings, with more donors than acceptors. The ring carbonyl O atom in (III), which represents the principal difference in potential hydrogen-bonding capability between this compound and the pair of compounds (I) and (II) reported here, does not participate in any hydrogen-bond formation. It is thus not easy to understand the difference in intermolecular hydrogen bonding between (I), (II) and (III).

Experimental

For the synthesis of (I) and (II), polyphosphoric acid (6.0 g) was added to a solution containing 0.1 mmol of either *N*-acetyl-2-allyl-*N*-benzyl-4-chloroaniline, for (I), or *N*-acetyl-2-allyl-*N*-benzyl-1-naphthylamine, for (II), in chloroform (3 ml). The mixtures were stirred at 370 K for 1–3 h until the reactions were complete, as judged by thin-layer chromatographic monitoring, and then brought to pH 7–8 using aqueous ammonia. Each mixture was extracted with ethyl acetate (3 × 50 ml) and the extracts were dried over anhydrous sodium sulfate. Concentration under reduced pressure gave the crude products, which were purified by column chromatography on silica gel using heptane–ethyl acetate (10:1 to 1:1 *v/v*) as eluent. Crystallization from heptane gave colourless crystals suitable for single-crystal X-ray diffraction. Analysis for (I): yield 33%, m.p. 378 K; MS (70 eV) *m/z* (%): 313 [*M*$^+$ (^{35}Cl), 74], 298 (35), 270 (100), 256 (93), 254 (38), 227 (3), 230 (26), 117 (69), 91 (52); elemental analysis found: C 72.6, H 6.5, N 4.5%; $C_{19}H_{20}ClNO$ requires: C 72.7, H 6.4, N 4.5%. Analysis for (II): yield 55%, m.p. 444 K; MS (70 eV) *m/z* (%): 329 (*M*$^+$, 82), 314 (8), 286 (28), 270 (100), 255 (57), 243 (17), 228 (12), 198 (28), 180 (11), 156 (27), 131 (24), 117 (48), 91 (20); elemental analysis found: C 83.9, H 6.9, N 4.3%; $C_{23}H_{23}NO$ requires: C 83.9, H 7.0, N 4.3%.

Table 1
Selected bond lengths (Å) for (II).

C1—C2	1.375 (5)	C6—C6a	1.421 (3)
C2—C3	1.409 (3)	C6a—C14a	1.377 (3)
C3—C4	1.366 (6)	C14a—C14b	1.423 (3)
C4—C4a	1.424 (5)	C14b—C1	1.419 (3)
C4a—C5	1.410 (3)	C4a—C14b	1.423 (3)
C5—C6	1.364 (4)		

Table 2
Selected torsion angles (°) for (I) and (II).

(I)		(II)	
N5—C4a—C12a—C12	0.3 (3)	N14—C14a—C6a—C7	5.7 (13)
C4a—C12a—C12—C11	−38.9 (4)	C14a—C6a—C7—C8	−50.5 (12)
C12a—C12—C11—C10a	−42.5 (3)	C6a—C7—C8—C8a	−33.8 (6)
C12—C11—C10a—C6a	92.0 (3)	C7—C8—C8a—C12a	87.5 (7)
C11—C10a—C6a—C6	1.2 (4)	C8—C8a—C12a—C13	4.7 (9)
C10a—C6a—C6—N5	−46.9 (3)	C8a—C12a—C13—N14	−55.5 (9)
C6a—C6—N5—C4a	−38.9 (3)	C12a—C13—N14—C14a	−31.1 (8)
C6—N5—C4a—C12a	91.9 (3)	C13—N14—C14a—C6a	87.3 (9)

Notes: the values for (II) refer to the major disorder component, form *A*. The corresponding values for the structural isomer *C* are fairly similar to those in isomer *A*: −9 (3), −37 (3), −39.7 (15), 94.9 (18), −2 (2), −48 (2), −34.5 (17) and 98 (2)°, respectively. A somewhat different pattern is apparent in the corresponding values for enantiomer *B*: 5 (3), −92 (2), 20.4 (18), 53 (2), 5 (3), −93 (2), 21.7 (18) and 53 (2)°, respectively.

Table 3
Selected torsion angles (°) for (III).

N16—C20—C25—C1	1.2 (10)	C6—C8—C13—C14	1.8 (9)
C20—C25—C1—C6	−68.9 (8)	C8—C13—C14—N1	−64.3 (8)
C25—C1—C6—C8	−4.2 (8)	C13—C14—N16—C20	−16.3 (8)
C1—C6—C8—C13	73.7 (7)	C14—N16—C20—C25	87.3 (8)

Notes: the atom numbering is that depicted in Fig. 1 of the original publication (Bocelli *et al.*, 2002), which was stated by the authors to be arbitrary, *i.e.* unrelated to the chemical numbering scheme. This is not the atom numbering given in the CIF retrieved from the CSD.

Refinement

$R[F^2 > 2\sigma(F^2)] = 0.055$	202 parameters
$wR(F^2) = 0.143$	H-atom parameters constrained
$S = 1.03$	$\Delta\rho_{max} = 0.48$ e Å^{-3}
3134 reflections	$\Delta\rho_{min} = -0.38$ e Å^{-3}

Compound (I)

Crystal data

$C_{19}H_{20}ClNO$	$V = 1595.97$ (9) Å^3
$M_r = 313.81$	$Z = 4$
Monoclinic, $P2_1/c$	Mo *K*α radiation
$a = 8.3396$ (3) Å	$\mu = 0.24$ mm^{-1}
$b = 21.7131$ (7) Å	$T = 120$ K
$c = 9.2010$ (3) Å	$0.12 \times 0.12 \times 0.08$ mm
$\beta = 106.683$ (2)°	

Data collection

Bruker–Nonius APEXII CCD camera on κ-goniostat diffractometer	20184 measured reflections
	3134 independent reflections
	2342 reflections with $I > 2\sigma(I)$
Absorption correction: multi-scan (*SADABS*; Sheldrick, 2007)	$R_{int} = 0.072$
$T_{min} = 0.962, T_{max} = 0.981$	

Compound (II)

Crystal data

$C_{23}H_{23}NO$	$V = 1754.57$ (15) Å^3
$M_r = 329.42$	$Z = 4$
Monoclinic, $P2_1/c$	Mo *K*α radiation
$a = 18.9549$ (10) Å	$\mu = 0.08$ mm^{-1}
$b = 9.8917$ (4) Å	$T = 120$ K
$c = 9.4354$ (5) Å	$0.40 \times 0.20 \times 0.16$ mm
$\beta = 97.348$ (3)°	

Data collection

Bruker–Nonius APEXII CCD camera on κ-goniostat diffractometer	23961 measured reflections
	3262 independent reflections
	2250 reflections with $I > 2\sigma(I)$
Absorption correction: multi-scan (*SADABS*; Sheldrick, 2003)	$R_{int} = 0.080$
$T_{min} = 0.959, T_{max} = 0.988$	

organic compounds

For (I), all H atoms were located in difference maps, and they were then treated as riding atoms in geometrically idealized positions, with C—H = 0.95 (aromatic), 0.98 (CH$_3$), 0.99 (CH$_2$) or 1.00 Å (aliphatic CH), and with U_{iso}(H) = kU_{eq}(C), where k = 1.5 for the methyl groups, which were permitted to rotate but not to tilt, and 1.2 for all other H atoms.

It was apparent from an early stage in the refinement of (II) that the molecules were subject to disorder. This disorder was modelled in terms of three isomeric forms occupying closely similar sets of atomic sites. The predominant isomeric form, containing atom O141 and denoted here as form A, has a methyl substituent at C11 in the aryl group and an R configuration at the stereogenic atom C8 (Fig. 2a). A second isomeric form, containing atom O441 and denoted here as form B, is the S enantiomer of form A (Fig. 2b), and the third isomer, containing atom O641 and denoted here as form C, is a structural isomer of form A, still with an R configuration at atom C58 but now with a methyl group at C59 rather than C61 (Fig. 2c). In each isomeric form of (II), all H atoms were added in calculated positions, based upon those found in (I). In form A, distance restraints were applied to several of the bonded distances in the azocine ring, thus C6A—C7 = 1.51 (1) Å, C7—C8 = 1.52 (1) Å, C8—C8A = 1.56 (1) Å, C8A—C12A = 1.39 (1) Å, C12A—C13 = 1.52 (1) Å and C13—N14 = 1.47 (1) Å. In each of forms B and C, the directly bonded intra-molecular distances and the one-angle 1,3-distances were all, with the exception of those involving methyl C atoms C381 and C581, restrained to take the same values as the corresponding distances in form A, subject for both types of distance to an s.u. value of 0.005 Å. The seven atoms of the methyl-substituted aryl ring were, in each form, restrained to be planar and the geometry at the methylated C atom in each such ring was subjected to distance restraints, with the C(*ipso*)—C(methyl) distances restrained to 1.47 (1) Å and the C(*ortho*)—C(methyl) distances restrained to 2.48 (1) Å on form C. The anisotropic displacement parameters for sets of partial-occupancy atoms occupying essentially the same physical space were constrained to be equal, and the displacement behaviour of atoms C4a, C34a, C54a and C591 was restrained to be approximately isotropic. The low-angle reflection ($\bar{1}11$) was found to have an unexpectedly low observed intensity, and consequently it was omitted from the final refinements. Finally, the site occupancies for the three isomeric disorder components were restrained to sum to 1.000 (1). On this basis, the disorder model had 386 parameters, 244 restraints and 3262 data, and the site occupancies for isomers A, B and C refined to 0.634 (6), 0.107 (3) and 0.260 (5), respectively.

An alternative four-component model was also investigated. In this model, the fourth component, denoted here as form D, was the S enantiomer of form C. Using distance restraints in form D entirely similar to those employed in the first model, but with a common isotropic displacement parameter for all non-H atoms in form D, this model had 461 parameters, 449 restraints and 3262 data. The site occupancy for isomer D refined to 0.010 (2), with only trivial changes in the site occupancies for the other three isomers. This very low occupancy means that the electron density associated with each atom in isomer D is significantly lower than the general background noise in the difference map. This consideration, combined with the data/parameter ratio for this model, led us to discard it in favour of the three-component disorder model, which is the structural model for (II) which is reported here.

For both compounds, data collection: *COLLECT* (Nonius, 1999); cell refinement: *DIRAX/LSQ* (Duisenberg *et al.*, 2000); data reduction: *EVALCCD* (Duisenberg *et al.*, 2003); program(s) used to solve structure: *SIR2004* (Burla *et al.*, 2005); program(s) used to refine structure: *SHELXL97* (Sheldrick, 2008); molecular graphics: *PLATON* (Spek, 2009); software used to prepare material for publication: *SHELXL97* and *PLATON*.

Supplementary data for this paper are available from the IUCr electronic archives (Reference: GG3233). Services for accessing these data are described at the back of the journal.

References

Allen, F. H. (2002). *Acta Cryst.* B**58**, 380–388.
Bernstein, J., Davis, R. E., Shimoni, L. & Chang, N.-L. (1995). *Angew. Chem. Int. Ed. Engl.* **34**, 1555–1573.
Bocelli, G., Catellani, M., Cugini, F. & Ferraccioli, R. (2002). *Arkivoc*, **3**(v), 120–126.
Burla, M. C., Caliandro, R., Camalli, M., Carrozzini, B., Cascarano, G. L., De Caro, L., Giacovazzo, C., Polidori, G. & Spagna, R. (2005). *J. Appl. Cryst.* **38**, 381–388.
Capelli, S. C., Albinati, A., Mason, S. A. & Willis, B. T. M. (2006). *J. Phys. Chem. A*, **110**, 11695–11703.
Claus, K. H. & Krüger, C. (1988). *Acta Cryst.* C**44**, 1632–1634.
Duisenberg, A. J. M., Hooft, R. W. W., Schreurs, A. M. M. & Kroon, J. (2000). *J. Appl. Cryst.* **33**, 893–898.
Duisenberg, A. J. M., Kroon-Batenburg, L. M. J. & Schreurs, A. M. M. (2003). *J. Appl. Cryst.* **36**, 220–229.
Fabbiani, F. P. A., Allan, D. R., Parsons, S. & Pulham, C. R. (2006). *Acta Cryst.* B**62**, 826–842.
Nonius (1999). *COLLECT*. Nonius BV, Delft, The Netherlands.
Sheldrick, G. M. (2003). *SADABS*. Version 2.10. University of Göttingen, Germany.
Sheldrick, G. M. (2007). *SADABS*. Version 2007/2. University of Göttingen, Germany.
Sheldrick, G. M. (2008). *Acta Cryst.* A**64**, 112–122.
Spek, A. L. (2009). *Acta Cryst.* D**65**, 148–155.
Traetteberg, M. (1966). *Acta Chem. Scand.* **20**, 1724–1726.